A numerical study of rotating convection during tropical cyclogenesis

Gerard Kilroy and Roger K. Smith *
Meteorological Institute, University of Munich, Munich, Germany

March 21, 2012

6A.8
*

1. INTRODUCTION

The present study was motivated by observations of one particular disturbance that was declared Tropical Storm Gaston on 1 September 2010 by the National Hurricane Center, but which was downgraded on 2 September to a tropical depression after data from the first PREDICT mission into the disturbance became available. During the weather briefings for the experiment, there was much speculation that the storm failed to redevelop because of its weak pouch that enabled dry air to penetrate its core. The presumption was that the dry air in the lower to middle troposphere would strengthen downdraughts from deep convection and flood the boundary layer with low entropy air from above. However, later analyses of the dropwindsonde data showed that the mission average low-level pseudo-equivalent potential temperature increased during the five days on which the storm was monitored (Smith and Montgomery, 2012). While some of this increase may have been due to the increase in sea surface temperature as the disturbance tracked westwards, there is certainly no evidence of a reduction on a day-to-day time scale that might have thwarted Gaston's redevelopment. These question then is: are there other aspects of the convection that might be influenced by the presence of dry air that might ultimately be detrimental to cyclogenesis?

Numerical model simulations show that when convection occurs in an environment of non-zero vertical vorticity, updraughts amplify the vorticity by the process of vortex-tube stretching (Hendricks *et al.* 2004, Saunders and Montgomery 2004, Montgomery *et al.* 2006, Nguyen *et al.* 2008, Rozoff 2007, Wissmeier and Smith 2011). Using a cloud model, Wissmeier and Smith (2011) showed that even moderately deep clouds can produce a large amplification (by one to two orders of magnitude) of the vertical component of absolute vorticity on time scales of an hour, and even for a background rotation rate typical of the undisturbed tropical atmosphere. The vorticity so produced has a maximum in the lower troposphere and persists long after the initial updraught has decayed. They showed also that the induced tangential wind speeds by a single updraught is typically no more than a few meters per second with a horizontal scale on the order of a kilometre, and would be barely detectable by normal measurement methods in the presence of an ambient wind field.

Over the years, the common perception that dry air generally enhances the strength of convective downdraughts has been challenged in one way or another by a number of authors (Brown and Zhang 1997, Tomkins 2001, Redelsperger *et al.* 2002, Sobel *et al.* 2004, Kuchera and Parker 2005, Rozoff 2007, Holloway and Neelin 2009, James and Markowski 2009, Minoru and Sugiyama 2010). For example, James and Markowski (2009) performed numerical experiments to determine the effects of dry air aloft on quasi-linear convective systems. Using idealised soundings of differing values of Convective Available Potential Energy (CAPE) and moisture content, they found that dry air aloft exerts detrimental effects on overall convective intensity, weakening both updraughts and downdraughts. Kuchera and Parker (2005) found also that dry mid-level air is not uniquely associated with strong downdraughts leading to damaging gust fronts.

The above findings motivate the question: if *convective* downdraughts are not strengthened by the presence of dry air, what aspects of the ensuing convection might be detrimental to tropical cyclogenesis? Is it simply the fact that mesoscale downdraughts are strengthened, or is it that by reducing the updraught strength, the dry air reduces the ability of the convection to amplify vorticity? It is the latter question that is a focus of the present study. As a necessary first step, we focus here on the effects of dry air on a single cloud updraught using thermodynamic soundings based on the data for ex-Gaston. A study of the more complex question concerning subsequent cloud merger is currently under way.

2. THE NUMERICAL MODEL

The numerical model used for this study is the three-dimensional cloud model of Bryan and Fritsch (2002) and Bryan (2002). The model incorporates a parametrisation scheme for warm rain processes as well as one for processes involving ice microphysics. The latter is Gilmore's Li-scheme, in which cloud water, rain water, cloud ice, snow and hail/graupel are predicted (Gilmore *et al.* 2004).

2.1. *Model configuration*

The experiments use the same model configurations as that of Experiment 9 from Wissmeier and Smith (2011), except the horizontal domain size and grid spacing are halved to give improved horizontal resolution of the cloud updraughts. The horizontal domain size is 25 km $\times$ 25 km with a uniform horizontal grid spacing of 250 m. The vertical domain extends to a height of 25 km with the vertical grid interval stretching smoothly from 120 m at the surface to 1000 m at the top.

2.2. *Initiation of convection*

Convection is initiated in a quiescent environment by a symmetric thermal perturbation with a horizontal radius of 5 km and a vertical extent of 1 km. The temperature excess has a maximum at the surface at the centre of the perturbation and decreases monotonically to zero at the perturbation's edge. The perturbation centre coincides with the centre of the domain. Table I shows the temperature perturbation used in the various experiments described here.

*Corresponding author address: Roger K. Smith, Meteorological Institute, University of Munich, Theresienstr. 37, 80333 Munich, Germany, Email: roger.smith@lmu.de

Exp #	Sounding Date	Sounding Time UTC	TPW kg m^{-2}	CAPE J kg^{-1}	CIN J kg^{-1}	ΔT K
1	5/9/10*	18:20	62.3	2770	40	2
2	5/9/10*	18:20	59.3	2770	40	2
3	5/9/10*	18:20	54.8	2770	40	2

Table I. Launch time and details of the ten experiments studied herein. CAPE averaged from the surface to 500 m in J Kg^{-1}, minimum CIN between the surface and 500 m in J Kg^{-1}, and total precipitable water (TPW) in kg m^{-2}. ΔT refers to the strength of the initial thermal perturbation. * Refers to an idealized profile created using dropsonde data from the given date and time as a basis.

2.2.1. *Experiments with idealised soundings*

A list of all soundings used is presented in Table I. The three experiments are designed to explore the role of moisture on the dynamics and thermodynamics of the ensuing updraught and downdraught. Experiment 1 uses an idealised sounding with piecewise-linear profiles of virtual potential temperature, θ_v, and mixing ratio, r. This sounding approximates that obtained from the dropsonde launched at 18:20 UTC on 5 September into ex-Tropical Storm Gaston, but has somewhat lower CAPE (2770 J kg^{-1} compared with 3500 J kg^{-1}). The observed sounding was made near the centre of the low-level circulation in a region of high total precipitable water (TPW), high CAPE and zero Convective Inhibition (CIN).

Experiment 1 serves as a control to compare with Experiments 2 and 3, which have decreasing amounts of mid-level moisture. The reduced moisture lowers the TPW values to 59.3 kg m^{-2} for Experiment 2 and 54.8 kg m^{-2} for Experiment 3. The temperature profile of both altered soundings is adjusted slightly to preserve the virtual temperature of the control sounding, ensuring that each sounding has identical CAPE.

The calculations are carried out on an f-plane with the Coriolis parameter $f = \zeta_o$, where $\zeta_o = 1.5 \times 10^{-4}$ s^{-1}. This value is typical of the vertical vorticity at low levels in Ex-Tropical Storm Gaston (Mark Boothe, personal communication).

3. RESULTS

3.1. *Convective cell evolution*

Figure 1 shows the cross sections of vertical velocity, w, and density temperature difference, dT_ρ, between the updraught and the environment for Experiments 1 and 3. The quantity dT_ρ is a measure of the buoyancy including the effects of water loading (Emanuel 1994, Chapter 2)

Table II gives details of the updraught and downdraught strength for all experiments. These details include the maximum density temperature difference between the updraught and the environment ($dT_{\rho\,max}$), the maximum liquid water content (q_{Lmax}), the maximum ice content ($q_{Ice\,max}$), the maximum density temperature difference ($dT_{\rho\ min}$) between the downdraught and the environment, and maximum difference in pseudo-equivalent potential temperature ($d\theta_{e\ min}$) between the downdraught and the environment at the surface.

In all three experiments, the flow evolution is similar to that described many times previously (see Wissmeier and Smith 2011, section 4.1). In brief, the updraught that forms the first convective cell is initiated by the buoyancy of the initial bubble. The updraught develops slowly at first, but increases rapidly in vertical extent and strength as additional buoyancy is generated by the latent heat release of condensation. Cloud water produced by condensation is carried aloft in the updraught, and if it ascends high enough it freezes, thereby generating additional buoyancy through the latent heat of fusion. A fraction of the condensate grows large enough to fall against the updraught as ice, snow or rain, and subsequently generates a downdraught.

The updraught in Experiment 1 attains a maximum value of 27.1 m s^{-1} at a height of 6.5 km after about 26 minutes (see Figure 1a and Table II). The updraught subsequently decays as a result of mixing with ambient air and water loading. The water loading initiates a downdraught that is cooled as a result of melting and sublimation. The cooling is aided by the partial evaporation of rain as it falls into unsaturated air below cloud base. Finally, a pool of cold air forms and spreads out near the surface.

3.2. *The effects of dry air aloft*

A comparison the values of w_{max} for Experiments 1, 2 and 3 in Table II shows that updraught is significantly weakened in Experiments 3 when moisture is removed from the lowest levels (i.e. below 2.5 km), but less so when these levels remain moist (Experiments 2). The updraughts in Experiments 2 and 3 have maximum values of 25 m s^{-1} and 16.5 m s^{-1} at heights of 4.7 and 2.8 km, respectively. Thus the presence of the environmental layer of dry air reduces the updraught strength as well as the altitude attained by the updraught, the reduction being most dramatic in Experiment 3. The foregoing reductions are a manifestation of the diminished updraught buoyancy (compare panels (b) and (d) in Figure 1).

The reduced buoyancy may be attributed to the entrainment of the drier air, which decreases the amount of water that condenses and therefore the amount of latent heat release. The effect is evident in a comparison of the liquid water and ice mixing ratios between the three experiments (see Table II). The maximum liquid water content is 10.1 g kg^{-1} in Experiment 2 and only 6.4 g kg^{-1} in Experiment 3, compared with 11.4 g kg^{-1} in Experiment 1. The lower liquid water content means also that there are fewer water particles to freeze, and therefore less generation of additional buoyancy above the freezing level by the latent heat of freezing. Note that in Experiment 1, a relatively large ice mixing ratio leads to a large vertical velocity maximum at a height of 6.5 km. In contrast, there are comparatively few ice hydrometeors in Experiment 3 as the cloud only ascends slightly above the freezing level, which is about 5.5 km high.

In Experiments 1-3, the strongest downdraught (9.6 m s^{-1}) occurs in Experiment 1, while the downdraughts become progressively weaker as the environment becomes drier (see Table II). The negative buoyancy of the downdraught characterized by $dT_{\rho\,min}$ diminishes also with increasing dryness, being -2.6 K in Experiment 1, -1.9 K in Experiment 2, and only -0.8 K in Experiment 3.

In the drier environment of Experiments 2 and 3, the negative vertical gradient of θ_e is much larger at low levels than in Experiment 1, especially just above 1 km, where the dry air is introduced. Thus, the weaker downdraughts in Experiment 3 are able to bring down low-θ_e air into the boundary layer with θ_e

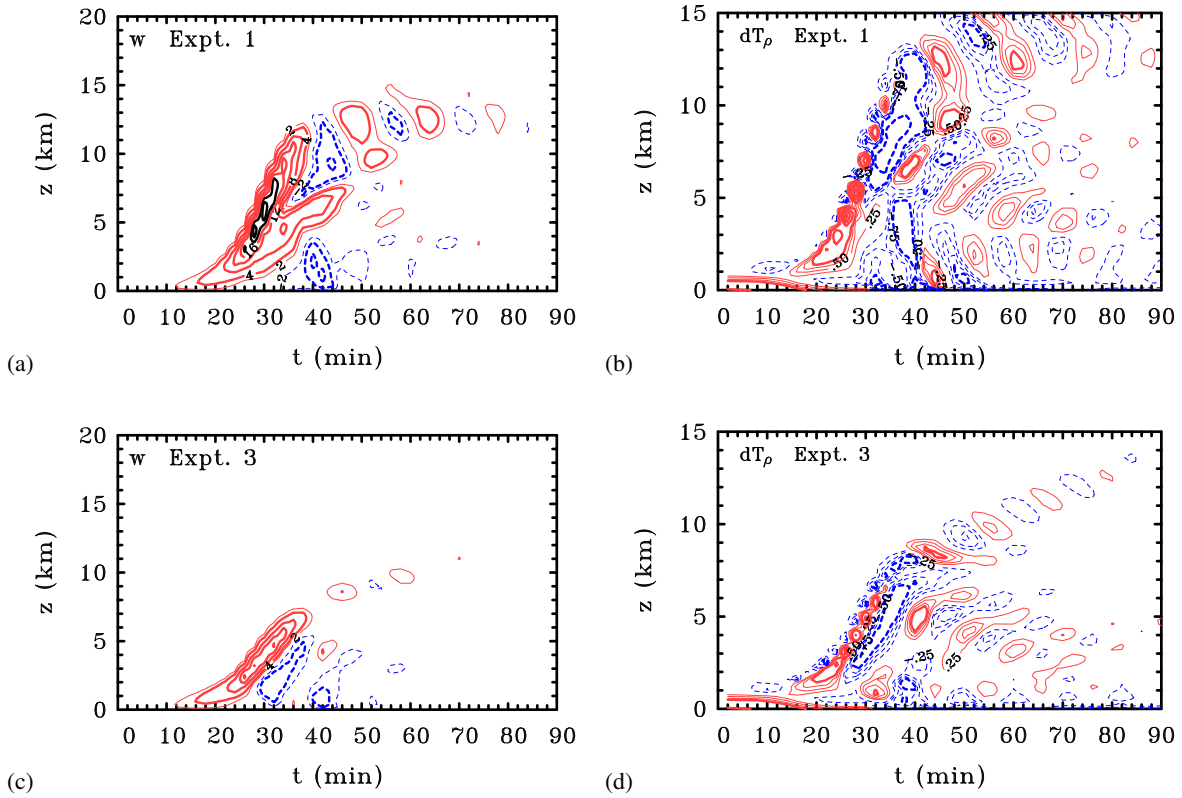

Figure 1. Height-time series of maximum vertical velocity, w, (left column) and density temperature difference between the updraught and its environment, dT_ρ, (right column) taken at the centre of the updraught in Experiments 1 and 3. Contour interval for w, thin contours 2 m s^{-1}, thick contours 4 m s^{-1}. Thick black contours show values above 20 m s^{-1} and are in intervals of 5 m s^{-1}. Solid/red contours show positive values, dashed/blue contours negative values. Thick black contours show values above 20 m s^{-1} and are in intervals of 5 m s^{-1}. Contour interval for dT_ρ: thin contours 0.25 K, 0.5 K, 0.75 K, thick contours 1 K.

Expt.	w_{max} m s^{-1}	$z(w_{max})$ km	w_{min} m s^{-1}	$z(w_{min})$ km	$q_{L\,max}$ g kg^{-1}	$q_{Ice\,max}$ g kg^{-1}	$dT_{\rho\,max}$ K	$z(dT_{\rho\,max})$ km	$dT_{\rho\,min}$ K	$d\theta_{e\ min}$ K
1	27.1	6.5	-9.6	1.3	11.4	8.6	4.4	4.0	-2.6	-21.0
2	25.0	4.7	-7.6	2.5	10.1	7.1	4.1	3.8	-1.9	-15.4
3	16.5	2.8	-6.9	2.2	6.4	2.2	2.4	3.2	-0.8	-20.2

Table II. Maximum vertical velocity (w_{max}) at the centre of the domain, the height of this maximum ($z(w_{max})$), minimum vertical velocity below 10 km (w_{min}) at the centre of the domain, the height of this minimum ($z(w_{min})$), the maximum liquid water content ($q_{L\,max}$) and the maximum ice content ($q_{Ice\,max}$) in Experiments 1-3. Listed also are the density perturbation temperature ($dT_{\rho\,max}$), the height of this maximum, the minimum surface density perturbation temperature ($dT_{\rho\,min}$), which indicates the strength of the low level cold pool, and the minimum surface pseudo-equivalent potential temperature depression ($d\theta_{e\ min}$).

values comparable to those in Experiment 1 (note that $d\theta_{e\ min}$ is -21 K in Experiment 1 and -20.2 K in Experiment 3: see Table II).

3.3. The amplification of ambient vertical vorticity

Since the pioneering study of Hendricks *et al.* (2004), there is growing evidence that all deep convection, and even convection of moderate vertical extent, produces a significant amplification of local vertical vorticity by vortex-tube stretching (Wissmeier and Smith 2011 and references). There is evidence also that this convectively-generated vorticity is important in both the genesis of tropical cyclones (e.g. Hendricks *et al.* 2004, Montgomery *et al.* 2006) and their intensification (e.g. Nguyen *et al.* 2008, Shin and Smith 2008, Fang and Zhang 2010). Such vorticity is able to interact with like-signed patches of vorticity produced by neighbouring convective cells, to be strengthened further by subsequent convection, and to be progressively axisymmetrized by the angular shear of the parent vortex as discussed in Montgomery *et al.* (2006) and Nguyen *et al.* (2008). If the most important effect of mid-level dry air on convective clouds is to reduce the updraught strength rather to increase the downdraught strength, is the detrimental effect of dry air on tropical cyclogenesis simply that it reduces the ability of the convection to locally amplify the ambient vertical vorticity?

Time-height cross sections of vertical vorticity for Experiments 1 and 3 are shown in Figure 2, and in the values for the maximum vertical vorticity (ζ_{max}) as a fraction of the background vorticity (ζ_1) in Table III. The maxima of ζ_{max}/ζ_1 in Table III and the time of their occurrence, $t_{\zeta_{max}}$, refer to the first convective updraught which forms along the axis.

The maximum amplification by the first updraught in Experiments 1-3 is about 43-44 times the background vorticity and occurs at the surface after about 24 minutes. Perhaps surprisingly, the magnitude of the amplification is insensitive to the maximum updraught strength or vertical extent of the cloud, although the deeper clouds produce an amplification of the vorticity through a deeper layer of the atmosphere.

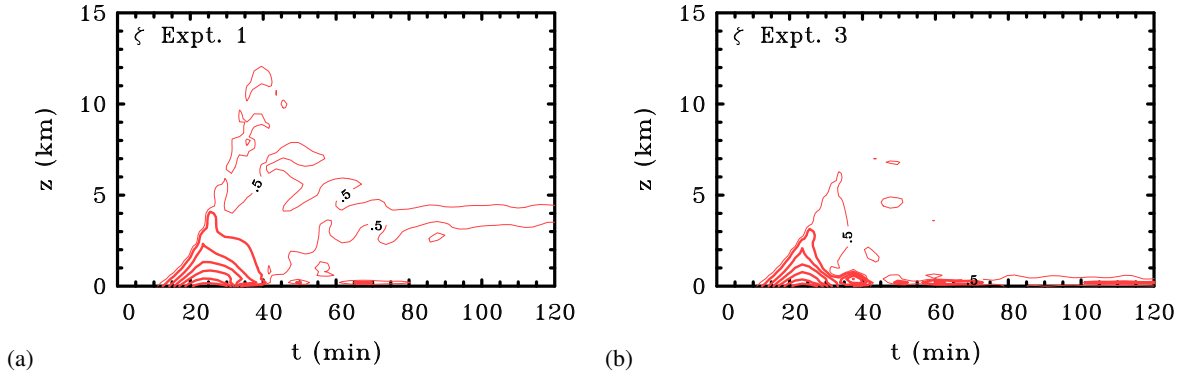

Figure 2. Height-time cross sections of maximum vertical component of relative vorticity taken in the centre of the updraught in Experiments 1 and 3. Contour interval = 1×10^{-3} s^{-1}. Solid/red contours show positive values, dashed/blue contours negative values. The thin solid curve shows the 0.5×10^{-3} s^{-1} contour.

Expt.	ζ_{max}/ζ_1	$t_{\zeta_{max}}$ min
1	44	26
2	44	26
3	43	24

Table III. The degree of amplification of the ambient vorticity by the first updraught cell (ζ_{max}/ζ_1) and the time ($t_{\zeta_{max}}$) at which it occurs.

4. CONCLUSIONS

We have described a series of numerical experiments designed to isolate the effects of dry air aloft on deep convection. The initial structure of vertical vorticity was idealized by assuming solid body rotation, but with a value characteristic of disturbances observed during the experiment.

The calculations do not support a common perception that dry air aloft produces stronger downdraughts and more intense outflows. Rather, the entrainment of dry air aloft was found to weaken both updraughts and downdraughts. Consistent with recent findings of Wissmeier and Smith (2011), growing convective cells amplify locally the ambient rotation at low levels by more than an order of magnitude and this vorticity persists long after the initial updraught has decayed.

Extending the findings of Wissmeier and Smith (2011), we showed that the degree of amplification is insensitive to the presence of dry air aloft. Nevertheless, the reduction in the depth of the strengthened rotation may be an important effect of dry air on the dynamics of tropical cyclogenesis.

References

Brown RG Zhang C. 1997: Variability of midtropospheric moisture and its effect on cloud-top height distribution during TOGA COARE. *J. Atmos. Sci.*, **54**, 27602774.

Bryan GH. 2002: An investigation of the convective region of numerically simulated squall lines. *Ph.D. thesis, The Pennsylvania State University*, 181 pp.

Bryan GH Fritsch JM. 2002: A benchmark simulation for moist nonhydrostatic numerical models. *Mon. Wea. Rev.*, **130**, 2917-2928.

Emanuel KA. 1994: Atmospheric convection. *Oxford University Press*, 580 pp.

Fang J Zhang F. 2010: Initial development and genesis of Hurricane Dolly (2008). *J. Atmos. Sci.*, **67**, 655-672.

Gilmore MS Straka JM Rasmussen EN. 2004. Precipitation and evolution sensitivity in simulated deep convective storms: comparisons between liquid-only and simple ice and liquid phase microphysics. *Mon. Wea. Rev.*, **132**, 1897-1916.

Hendricks EA Montgomery MT Davis CA. 2004: On the role of "vortical" hot towers in formation of tropical cyclone Diana (1984). *J. Atmos. Sci.*, **61**, 1209-1232.

Holloway CE Neelin JD. 2009: Moisture vertical structure, column water vapor, and tropical deep convection. *J. Atmos. Sci.*, **66**, 16651683.

James, Richard P Markowski PM., 2009: A numerical investigation of the effects of dry air aloft on deep convection. *Mon. Wea. Rev.*, **138**, 140-161.

Kuchera EL Parker MD. 2006: Severe convective wind environments. *Wea. Forecasting*, **21**, 595-612.

Minoru C Sugiyama M. 2010: A cumulus parameterization with state-dependent entrainment rate. Part I: Description and sensitivity to temperature and humidity profiles. *J. Atmos. Sci.*, **67**, 21712193.

Montgomery MT Nicholls ME Cram TA Saunders AB. 2006: A vortical hot tower route to tropical cyclogenesis. *J. Atmos. Sci.*, **63**, 355-386.

Nguyen SV Smith RK Montgomery MT. 2008: Tropical-cyclone intensification and predictability in three dimensions. *Q. J. R. Meteorol. Soc.*, **134**, 563-582.

Redelsperger JL Parsons DB Guichard F. 2002: Recovery processes and factors limiting cloud-top height following the arrival of a dry intrusion observed during TOGA COARE. *J. Atmos. Sci.*, **59**, 24382457.

Rozoff CM 2007: Aspects of moat formation in tropical cyclone eyewall replacement cycles. *Ph.D. thesis, Colorado State University*, 165 pp.

Saunders and Montgomery MT. 2004: A closer look at vortical hot towers within a tropical cyclogenesis environment. Colorado State University, Atmospheric Science Bluebook No. 752.

Shin S Smith RK. 2008 Tropical-cyclone intensification and predictability in a minimal three-dimensional model. **134**, 1661-1671.

Smith RK Montgomery MT. 2012: Observations of the convective environment in developing and non-developing tropical disturbances. *Q. J. R. Meteorol. Soc.*, **138**, (in press).

Sobel AH. Yuter SE Bretherton CS Kiladis GN. 2004: Large-scale meteorology and deep convection during TRMM KWAJEX. *Mon. Wea. Rev.*, **132**, 422444.

Tompkins AM. 2001: Organization of tropical convection in low vertical wind shears: The role of water vapor. *J. Atmos. Sci.*, **58**, 529545.

Wissmeier U Smith RK. 2011: Tropical-cyclone convection: the effects of ambient vertical vorticity. *Q. J. R. Meteorol. Soc.*, **137**, 845-857.